[5] J. C. Vartuli, K. D. Schmitt, C. T. Kresge, W. J. Roth, M. E. Leonowicz, S. B. McCullen, S. D. Hellring, J. S. Beck, J. L. Schlenker, D. H. Olson, E. W. Sheppard, *Chem. Mater.* **1994**, *6*, 2317.
[6] X. S. Zhao, G. Q. Lu, *J. Phys. Chem. B* **1998**, *102*, 1556.
[7] M. H. Lim, A. Stein, *Chem. Mater.* **1999**, *11*, 3285.
[8] S. Burkett, S. D. Sims, S. Mann, *Chem. Commun.* **1996**, 1367.
[9] S. Mann, S. L. Burkett, S. A. Davis, C. E. Fowler, N. H. Mendelson, S. D. Sims, D. Walsh, N. T. Whilton, *Chem. Mater.* **1997**, *9*, 2300.
[10] J. Joo, T. Hyeon, J. Hyeon-Lee, *Chem. Commun.* **2000**, 1487.
[11] S. Inagaki, S. Guan, T. Ohsuna, O. Terasaki, *Nature* **2002**, *416*, 304.
[12] D. E. Aspnes, *Am. J. Phys.* **1982**, *50*, 704.
[13] D. Grosso, A. R. Balkenende, P. A. Albouy, M. Lavergne, L. Mazerolles, F,. Babonneau, *J. Mater. Chem.* **2000**, *10*, 2085.
[14] Q. Huo, D. I. Margolese, U. Ciesla, D. G. Demuth, P. Feng, T. E. Gier, P. Sieger, A. Firouzi, B. F. Chmelka, F. Schüth, G. D. Stucky, *Chem. Mater.* **1994**, *6,* 1176.

Diameter-Controlled Growth of Single-Crystalline In_2O_3 Nanowires and Their Electronic Properties**

By *Chao Li*, *Daihua Zhang*, *Song Han*, *Xiaolei Liu*, *Tao Tang*, and *Chongwu Zhou**

One-dimensional nanostructured systems have recently attracted much attention due to their novel properties and potential applications in numerous areas such as nanoscale electronics and photonics.[1–7] Nanowires of various compositions have been synthesized using a wide variety of methods including chemical vapor deposition (CVD),[1–4] laser ablation,[5–7] and electrochemical deposition.[8] These efforts have led to the successful growth of many semiconductive nanowires including Ge,[1] ZnO,[2] Si,[4–5] GaN,[9] and GaAs,[10] which were then employed to construct such exciting systems as nanowire integrated systems[11] and nanolasers.[12]

Parallel to the success with group IV and III–V compound semiconductor nanowires, semiconducting oxide nanowires such as ZnO,[2] CdO, and In_2O_3 are becoming increasingly important. Among them, In_2O_3 is a wide-bandgap transparent semiconductor (with a direct bandgap around 3.6 eV and an indirect bandgap around 2.5 eV), and In_2O_3 in the bulk form has been widely used in solar cells and organic light-emitting diodes.[13–14] More importantly, In_2O_3 films have been demonstrated to work as ultra-sensitive toxic-gas detectors,[15] with detection levels down to 5 ppm for NO_2, due to the surface interaction and electron transfer between NO_2 molecules and In_2O_3 surface. In_2O_3 in the nanowire form is expected to offer enhanced sensitivity and also improved response time due to the enhanced surface-to-volume ratio. It is therefore important to be able to synthesize In_2O_3 nanowires with highly uniform geometries, preferentially in the single-crystalline form, for electronic properties studies and potential sensor applications. Several methods were developed in the past to grow In_2O_3 nanowires. For example, polycrystalline In_2O_3 nanowires were grown by electrodepositing indium into an anodized alumina template and subsequent oxidation.[8] More recently, single-crystalline In_2O_3 nanowires were grown by a rapid heating process from indium grains in a mixture of Ar and O_2;[16] however, this method yields nanowires with a wide diameter distribution due to the lack of a diameter-control mechanism. The same is also true for semiconductive oxide nanobelts reported recently.[17] This drawback can be overcome by using the vapor–liquid–solid (VLS) growth approach,[5] where the nanowire diameters can be controlled by the catalyst nanoparticle size.[18] Here, we report an efficient route for the synthesis of single-crystalline In_2O_3 nanowires via the VLS mechanism, where the In vapor was generated by laser ablation of an indium-containing target. While catalysts made of a thin gold film produced In_2O_3 nanowire with a broad diameter distribution, excellent diameter control was achieved by using monodispersed gold clusters as the catalyst. Detailed transmission electron microscopy (TEM) examination confirmed the composition of our nanowires and reveals our nanowires exhibit narrow diameter distributions peaked at 10, 20, and 30 nm, respectively. In_2O_3 nanowire field-effect transistors were also made for the first time with on/off ratios up to 1000.

First, In_2O_3 nanowires were grown using Si/SiO_2 substrates covered with 20 Å gold films as the catalyst. The substrates were placed into a quartz tube at the downstream end of a furnace, while an InAs target was placed at the upper stream of the furnace and later on ablated to supply the In vapor. During the laser ablation, the chamber was maintained at 220 torr, 770 °C with a constant flow of 150 standard cubic centimeters per minute (sccm) of Ar mixed with 0.02 % O_2. The typical reaction time used was about 35 minutes. After cooling down, the samples were characterized using scanning electron microscopy (SEM), transmission electron microscopy (TEM), selected-area electron diffraction (SAED), and X-ray diffraction (XRD). The nanowire diameters were usually determined using TEM and the lengths were measured from SEM images.

Figure 1a shows a typical SEM image of In_2O_3 nanowires grown on the Si/SiO_2 substrate with evaporated Au catalysts. These nanowires covered the whole substrates and appeared to be straight. Detailed TEM and SEM examination show that these nanowires have diameters in the range of 30–50 nm and lengths exceeding 3 μm, indicating an aspect ratio of more than 100:1. XRD patterns of such nanowire samples were utilized to examine the crystal structure of the nanowires. All samples showed similar XRD patterns, indicating the nanowires' high crystallinity. There are three major diffraction peaks, as showed in Figure 1b. They can be indexed to the (222), (440), and (400) crystal planes of a cubic structure of

[*] Prof. C. Zhou, C. Li, D. Zhang, S. Han, X. Liu, T. Tang
Department of Electrical Engineering–Electrophysics
University of Southern California
Los Angeles, CA 90089-0271 (USA)
E-mail: chongwuz@usc.edu

[**] We thank Dr. Jie Han and Dr. Meyya Meyyapan at NASA Ames Research Center for valuable technical discussions. Prof. Edward Goo and the USC Microscope Center are acknowledged for the use of their facilities. We thank Prof. Martin Gundersen and Dr. Xiaodong Zhang for their help with the laser ablation process. This work is supported by USC, a Powell award, NASA contract NAS2-99092, NSF CAREER award, NSF NER program and a Zumberger award.

  0935-9648/03/0201-0143 $ 17.50+.50/0

ADVANCED MATERIALS

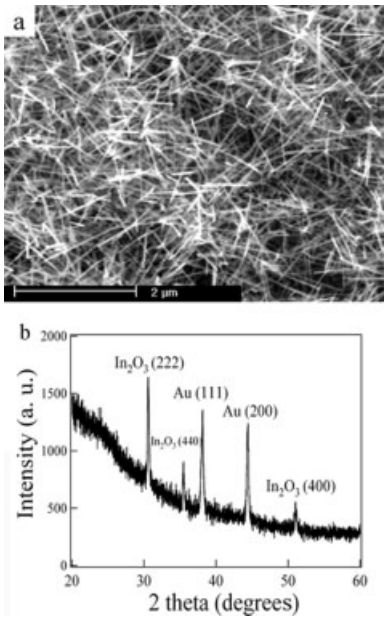

Fig. 1. a) SEM image of In_2O_3 nanowires grown by laser ablation on a Si/SiO_2 substrate coated with 20 Å Au film. b) XRD pattern of In_2O_3 nanowires on a Si/SiO_2 substrate. Indices of the peaks are marked above the peaks. Au peaks come from the catalyst.

bulk In_2O_3 with a cell constant of $a = 1.01$ nm.[19] Two gold peaks from the Au catalysts can also be identified; however, no diffraction peaks from InAs can be found in any of our samples. Although this laser ablation process generated both In and As vapors, we believe O_2 is more reactive than As, and hence In_2O_3 instead of InAs was found to be the final product. Energy-dispersive X-ray spectroscopy (EDS) was also performed to analyze the composition of our nanowires and no peaks corresponding to As were detected down to the limit of our equipment.

Despite the above-mentioned success, direct and precise control over the In_2O_3 nanowire diameter is still highly desired. Furthermore, nanowires with diameters below 30 nm are also necessary in order to make nanowire-based field effect transistors because of the finite depth a gate electric field can penetrate. This was achieved by using monodispersed gold clusters instead of the evaporated gold film as the catalysts. The idea is based on the VLS growth mechanism, where the In vapor first diffuses into the gold catalytic particles, and grows out and reacts with O_2 to form In_2O_3 once the In/Au alloy reaches supersaturation. Continued addition of In into the In/Au nanoparticle feeds the In_2O_3 growth and eventually the diameter of the In_2O_3 nanowire is directly linked to the catalytic particle size. This diameter-control feature is rather unique to the VLS mechanism, in contrast to the lack of control with the rapid heating process. Three types of clusters were used, with diameters around 10, 20, and 30 nm, respectively. These nanoclusters were dispersed onto a Si/SiO_2 substrate following previously published work[18] and atomic force microscopy (AFM) was performed to confirm these nanoclusters distributed uniformly across the surface. Abundant In_2O_3 nanowires were produced all over the substrates following the same laser ablation conditions described above. Figure 2a is a detailed TEM examination of a single In_2O_3 nanowire made from 10 nm Au cluster. The Au/In alloy particle, with a diameter around 10 nm, can be clearly seen at

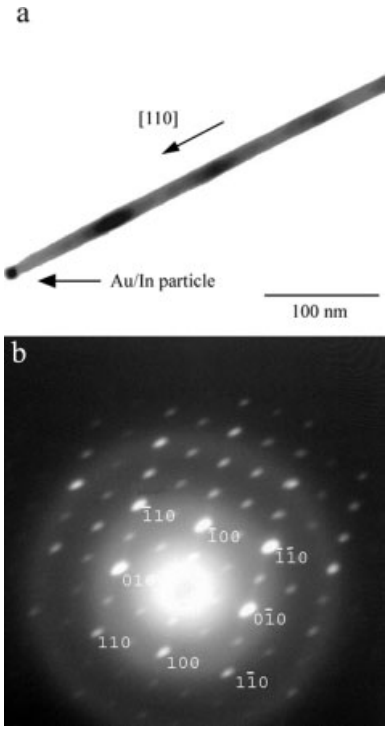

Fig. 2. a) TEM image of an In_2O_3 nanowire with a catalyst particle at the very tip. The scale bar is 100 nm. b) Electron diffraction pattern of the In_2O_3 nanowire indicating the single-crystalline nature, and the growth direction is along [110].

the very tip of the nanowire. The electron scattering cross section of the gold atom is larger than that of In_2O_3, and hence the Au/In alloy nanoparticle appears darker than the In_2O_3 nanowire in Figure 2a. The In_2O_3 appears rather homogeneous without any domain boundaries, indicating the single-crystalline nature of our material, as expected from the VLS growth mechanism. The nanowire diameter (~10 nm) is apparently consistent with the diameter of the catalytic particle. The highly crystalline nature of our In_2O_3 nanowires was further confirmed by selective-area electron diffraction. Figure 2b shows an SAED pattern, recorded perpendicular to a nanowire long axis. By analysis the SAED pattern, we can estimate the nanowire takes a cubic crystal structure with a lattice constant of 1.03 nm, also consistent with that of the bulk In_2O_3 ($a = 1.01$ nm).[19] In addition, indexing the pattern demonstrates that the [110] direction is the nanowire growth direction. We performed TEM examination and SAED over many nanowires made from both Au film and cluster samples and also at different location along each nanowire. Similar diffraction pattern have always been observed.

The above-mentioned growth and characterization method allowed us to convincingly establish the diameter-controlled growth of In_2O_3 nanowires by using three kinds (10 ± 1.5 nm, 20 ± 2.0 nm, 30 ± 3.0 nm) of Au clusters as the catalytic parti-

  0935-9648/03/0201-0144 $ 17.50+.50/0

cles. Figures 3a, c, and e are typical TEM images of In_2O_3 nanowires grown from these clusters. A direct connection between the catalytic particle size and the nanowire diameter

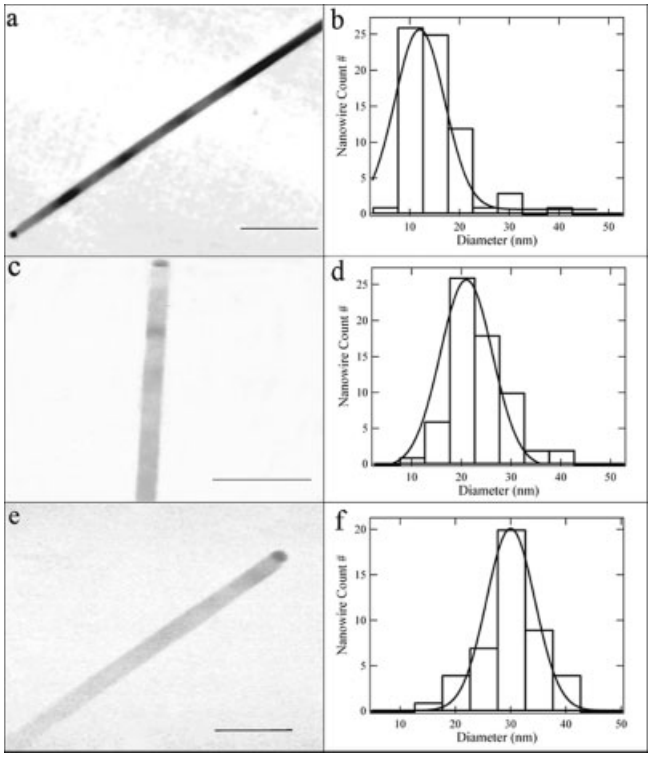

Fig. 3. TEM images of typical In_2O_3 nanowires grown using monodispersed Au clusters of a) 10 nm, c) 20 nm, e) 30 nm in diameter, respectively. Scale bars are 100 nm for all three images. Corresponding histograms for the nanowire diameter distributions are plotted in b), d), f), respectively. The solid lines correspond to Gaussian fits.

is clearly visible. TEM inspection was performed over fifty nanowires for each kind of gold clusters to generate the wire diameter distribution shown in Figures 3b, d, and f. The mean nanowire diameters are 10.9 ± 1.1 nm, 20.6 ± 2.5 nm, 30.1 ± 2.4 nm, respectively. From these histograms, we can see the width of the nanowires mirrors the colloid catalyst particle size very well.

The ability to produce nanowires of small and uniform diameters is especially important for fundamental studies such as their electronic properties. In_2O_3 is known to be non-stoichiometric n-type semiconductor in the bulk form due to the O_2 deficiency.[15] To our best knowledge, we have made the first In_2O_3 nanowire field-effect transistors (FETs). A degenerately doped silicon wafer covered with 500 nm SiO_2 was used as the substrate, on which In_2O_3 nanowires of 10 nm in diameter were deposited. Photolithography was performed, followed by evaporating Ti/Au to contact both ends of the nanowires. A typical SEM image of our device is shown in Figure 4b inset, indicating a channel length of 3 μm between the source and drain electrodes. The silicon substrate was used as a back gate. Figure 4a shows a family of current–voltage (I–V_{ds}) curves of an In_2O_3 FET under various gate biases (V_g). The I–V_{ds} curve for $V_g = 0$ V displays a linear resistance

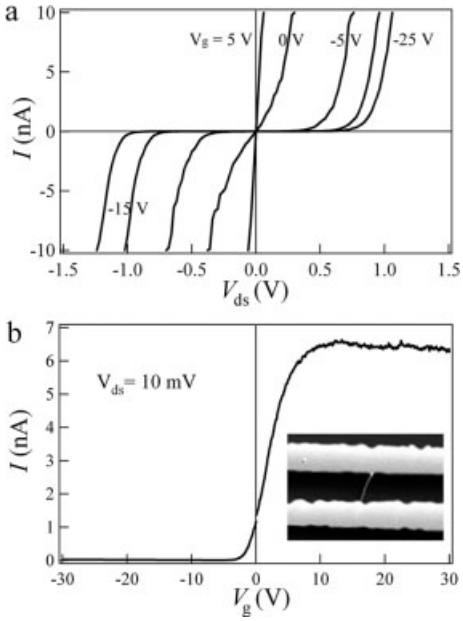

Fig. 4. a) I–V curves recorded on an In_2O_3 nanowire of 10 nm in diameter with the gate voltage varying from 5 V to –25 V, indicating n-type semiconductor behavior. b) I–V_g data of the same device at $V_{ds} = 10$ mV. The on/off ratio is ~1000; inset: an SEM image of the nanowire between the Ti/Au source and drain electrodes.

of 70 MΩ with enhanced conductance at higher bias, indicating the electrical contacts are not completely ohmic. However, a positive gate bias of 5 V led to substantially enhance conduction (~6 MΩ) and also a linear I–V curve, indicating n-type semiconductor behavior. This is further confirmed as a negatively increasing gate bias gradually reduced the conduction. With $V_g = -25$ V, the conduction was almost completely suppressed between $V_{ds} = -1.0$ V and $V_{ds} = 0.8$ V. Figure 4b shows an I–V_g curve measured at $V_{ds} = 10$ mV, where V_g was swept from –30 V to 30 V. We can see the nanowire was conductive at $V_g = 0$ V, but can be depleted with a V_g below –4 V. Current saturation was observed for $V_g > 10$ V, as the conduction in this regime was limited by the contact resistance between the nanowire and the electrodes. A slight decrease in the current was further observed for $V_g > 15$ V. This is likely due to a slight degradation of the carrier mobility under high gate bias, which brought electrons closer to the nanowire/SiO_2 interface and therefore led to enhanced electron scattering with the boundary of the nanowire and interface traps. Similar phenomena were observed with nanotubes transistors before.[20] The on/off ratio of our device can reach as high as 1000. From these data, it is possible to estimate the electron concentration and the mobility.[21,22] The total charge on the nanowire is $Q = C \cdot V_{g,t}$, where C is the nanowire capacitance and $V_{g,t}$ the threshold voltage necessary to completely deplete the wire. The capacitance of nanowire is given by $C \approx 2\pi\epsilon\epsilon_0 L/\ln(2h/r)$, where ϵ is the dielectric constant, h is the thickness of the silicon oxide layer, and r and L are the radius and length of the In_2O_3 nanowire. Using $L = 3$ μm, $r = 5$ nm, $h = 500$ nm, and $\epsilon = 3.9$, we deduce a one-dimensional electron density of $n = Q/eL \approx 1.02 \times 10^7$ cm^{-1} from

  0935-9648/03/0201-0145 $ 17.50+.50/0

ADVANCED MATERIALS

$V_{g,t} = -4$ V. The mobility of the electrons can also be deduced from the transconductance of the FET. In the linear regime, it is given by $dI/dV_g = \mu(CL^{-2})V_{ds}$. From Figure 4b, we get $dI/dV_g = 9.7 \times 10^{-10}$ AV^{-1} at $V_{ds} = 10$ mV, corresponding to an electron mobility of 71 cm^2 V^{-1} s^{-1}.

In summary, high-quality indium oxide nanowires were synthesized using a laser ablation technique, and their composition and single-crystalline structures were confirmed using XRD, TEM, and SAED. Precise control over the nanowire diameter was achieved by using monodispersed gold clusters as the catalytic nanoparticles. The growth can be explained by the VLS mechanism. FETs were also fabricated based on these nanowires. Detailed electrical measurements confirmed that the indium oxide nanowires were n-type semiconductors, and the on/off ratio of the field effect transistor can reach up to 1000. We believe these nanowires could be used as active sensing materials and also building blocks for nanoelectronics.

Experimental

Si/SiO_2 substrates were cleaned in acetone and isopropanol. For growth with thin gold films as the catalyst, the substrates were coated with 20 Å Au using a Temescal e-beam evaporator, followed by baking in Ar atmosphere for half an hour to break the Au films into nanoparticles. For growth with nanoclusters as the catalyst, the substrates were coated with a layer of gold clusters (Ted Pella). Three kinds of clusters with diameters of 10±1.5 nm, 20±2.0 nm, 30±3.0 nm were used, and atomic force microscopy (Digital Instruments Dimension 3100) was performed to confirm these nanoclusters distributed uniformly across the surface. The substrates were loaded into a quartz tube at the downstream end of a furnace, and an InAs (Alfa Aesar, 99.999 %) target was placed at the upper stream of the furnace. The system was first pumped to a base pressure below 1 millitorr, and then Ar mixed with 0.02 % O_2 was flown through the system at a rate of 150 sccm, while the InAs target was ablated to supply the indium vapor. During the laser ablation process, the chamber was maintained at 220 torr, 770 °C. A pulsed Nd:YAG laser (Continuum) ($L = 532$ nm) with repetition rate of 10 Hz, and a pulse power of 1.0 W was used. The typical reaction time used was about 35 min. After the furnace cooled down to room temperature, light gray materials were found on the surface of the substrate.

The crystal structure of the nanowires was characterized using XRD (Rigaku RV - 200) and SAED (Phillips, 420 operated at 120 Kev). The nanowire diameters were usually determined from TEM (Phillips, 420 operated at 120 Kev) and the lengths were measured from SEM (Phillips XL30 operated at 15 Kev) images.

For electronic transport studies In_2O_3 nanowires of 10 nm in diameter were sonicated for 1 h in isopropanol, and then several drops were deposited onto a degenerately doped silicon wafer covered with 500 nm SiO_2. Photolithography was performed, followed by evaporating Ti/Au to contact both ends of the nanowires. Devices with a single In_2O_3 nanowire between the source and drain electrodes were chosen for further studies after a thorough SEM inspection. The electrical measurements were carried out using a semiconductor parameter analyzer (Agilent 4156B).

Received: July 25, 2002
Final version: November 11, 2002

[1] Y. Wu, P. Yang, *Chem. Mater.* **2000**, *12*, 605.
[2] M. H. Huang, Y. Wu, H. Feick. N. Tran, E. Weber. P. Yang, *Adv. Mater.* **2001**, *13*, 113.
[3] J. Kong, C. Zhou, A. Morpurgo, H. T. Soh, C. F. Quate, C. Marcus, H. Dai, *Appl. Phys. A* **1999**, 69, 305.
[4] Y. Cui, L. J. Lauhon, M. S. Gudiksen, J. Wang, C. M. Lieber, *Appl. Phys. Lett.* **2001**, 78, 2214.
[5] J. T. Hu, T. W. Odom, C. M. Lieber, *Acc. Chem. Res.* **1999**, *32*, 435.
[6] X. Duan, C. M. Lieber, *J. Am. Chem. Soc.* **2000**, *122*, 188.
[7] A. M. Morales, C. M. Lieber, *Science* **1998**, *279*, 208.
[8] M. J. Zheng, L. D. Zhang, G. H. Li, X. Y. Zhang. X. F. Wang, *Appl. Phys. Lett.* **2001**, *79*, 839.
[9] a) Y. Huang, X. Duan, Y. Cui, C. M. Lieber, *Nano Lett.* **2002**, *2*, 101. b) C. C. Chen, C. C. Yeh, *Adv. Mater.* **2000**, *12*, 738. c) J. Zhu, S. Fan, *J. Mater. Res.* **1999**, *14*, 1175. d) J. Kim, H. So, J. Park, J. Kim, J. Kim, C. Lee, S. Lyu, *Appl. Phys. Lett*. **2002**, *80*, 3548.
[10] X. F. Duan, C. M. Lieber, *Adv. Mater.* **2000**, *12*, 298.
[11] Y. Huang, X. Duan, Y. Cui, L. Lauhon, K. Kim, C. M. Lieber, *Science* **2001**, *294*, 1313.
[12] M. Huang, S. Mao, H. Feick, H. Yan, Y. Wu, H. Kind, E. Weber, R. Russo, P. Yang, *Science* **2001**, *292*, 1897.
[13] K. Sreenivas, T. S. Rao, A. Mansingh, *J. Appl. Phys.* **1985**, *57*, 384.
[14] Y. Shigesato, S. Takaki, T. Haranoh, *J. Appl. Phys.* **1992**, *71*, 3356.
[15] a) J. Tamaki, C. Naruo, Y. Yamamoto, M. Mastuoka, *Sens. Actuators B* **2002**, *83*, 190. b) D. E. Williams, *Sens. Actuators B* **1999**, *57*, 1. c) M. Liess, *Thin Solid Films* **2002**, *410*, 183.
[16] X. S. Peng, G. W. Meng, J. Zhang, X. F. Wang, Y. W. Wang, C. Z. Wang, L. D. Zhang, *J. Mater. Chem.* **2002**, *12*, 1602.
[17] Z. W. Pan, Z. R. Dai, Z. R. Wang, Science **2001**, *291*, 1947.
[18] M. S, Gudiksen, J. Wang, C. M. Lieber, *J. Phys. Chem. B* **2001**, *105*, 4062.
[19] R. W. G. Wyckoff, *Crystal Structures*, Interscience, New York **1968**.
[20] S. J. Tans, A. R. M. Verschueren, C. Dekker, *Nature* **1998**, *393*, 49.
[21] R. Martel, T. Schmidt, H. R. Shea, T. Hertel, P. Avouris, *Appl. Phys. Lett.* **1998**, *73*, 2447.
[22] C. Zhou, J. Kong, E. Yenilmez, H. Dai, *Science* **2000**, *290*, 1552.

An Unusual Electrochromic Device Based on a New Low-Bandgap Conjugated Polymer**

By *Hong Meng*, *Derald Tucker*, *Sterling Chaffins*, *Yongsheng Chen*, *Roger Helgeson*, *Bruce Dunn*, and *Fred Wudl**

Over the past few years, electrochromic devices (ECDs) using electrochemically active conjugated polymers have been widely investigated.[1] Interest in these materials is due to their advantageous properties such as low fabrication cost, processibility, and dynamic, color-tunable "smart windows".[1,2] Conjugated polyheterocyclic polymers, such as polyanilines, polypyridines, polypyrroles, polythiophenes, and in particular, poly(3,4-ethylenedioxythiophene) (PEDOT) and its derivatives have been studied as electrochromic materials.[3,4] These materials provide color changes within the visible spectrum, and some exhibit electrochromicity, changing from a transparent doped state to a colored neutral state.[4] As a decrease of absorption in the transparent doped state is accompanied by an increase of absorption in the infrared region, the application of a conducting-polymer-based "smart window" can be extended to infrared ranges.[5] Infrared modulation devices show great potential in devices such as a vari-

[*] Prof. F. Wudl, Dr H. Meng, Dr. S. Chaffins, Dr. Y. Chen, Dr. R. Helgeson
Department of Chemistry and Biochemistry
Exotic Materials Institute
University of California at Los Angeles
Los Angeles, CA 90095-1569 (USA)
E-mail: wudl@chem.ucla.edu
Dr. D. Tucker, Prof. B. Dunn
Department of Materials Science and Engineering
Exotic Materials Institute
University of California at Los Angeles
Los Angeles, CA 90095-1569 (USA)

[**] We thank the U.S. Air Force Office of Scientific Research for support through F49620-00-1-0103 and a MURI from the U.S. Army Research Office through DAAD19-99-1-0316.

  0935-9648/03/0201-0146 $ 17.50+.50/0